

# Application of a MicroFlown as a low-cost level-sensor

J. van Honschoten, J. van Baar, H.E. de Bree, T. Lammerink, G. Krijnen, M. Elwenspoek

MicroMechanical Transducers group, MESA Research Institute, University of Twente  
P.O. Box 217, 7500 AE Enschede, The Netherlands.

Email: j.w.vanhonschoten@el.utwente.nl

## Abstract

In this abstract we present a novel "spirit level"-sensor derived from a well-known thermal flow-sensor. The operation principle is based on the temperature difference of two identical heaters, caused by buoyancy of air. Heating as well as temperature sensing of the structures is carried out using temperature dependent platinum resistors. Due to its simplicity the sensor is easily fabricated in silicon micro-machining technology. Theory describing the sensor is presented. First experiments, using DC signals only, show an adequate sensitivity though high accuracy operation is hampered by thermal drift.

**Keywords:** Spirit level, vial, Microflown, thermal gravity sensor.

## Introduction

A spirit level (or vial) is an instrument that can detect if an object is placed horizontal. It is a widely used instrument that normally consists of an air bubble in a fluid. In Figure 1 the two most common realisations are shown. The accuracy of these devices is about 2 to 30 arc-minutes. Various implementations of vials have been investigated in the past, see e.g. [1] and [2]. Although for most applications bubble vials are the tools of first choice some applications may require or benefit from small sized, solid state level sensors.

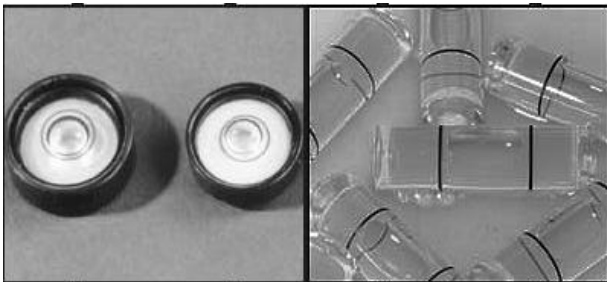


Figure 1 Left: circular vials, right tubular vials

The vial discussed here consists of two heaters with platinum wires on top. These

wires form resistors which are used to generate electrically heat. Simultaneously the resistors are used as temperature sensors exploiting the temperature resistance effect. Heat induced self-flow (or buoyancy) of the heated wires will cause a temperature difference of the two wires. This temperature difference is resolved by the temperature dependence of the resistors giving an output voltage deviating from zero for none level orientations. The realisation is well known: the sensing element is the same as that of a mass flow sensor [3], a Microflown [4] (particle velocity microphone), or even an accelerometer [5]. For the latter two patents have been filed recently. It is quite remarkable that with only two heated wires, but in different set-ups it is possible to detect angle, velocity, or acceleration.

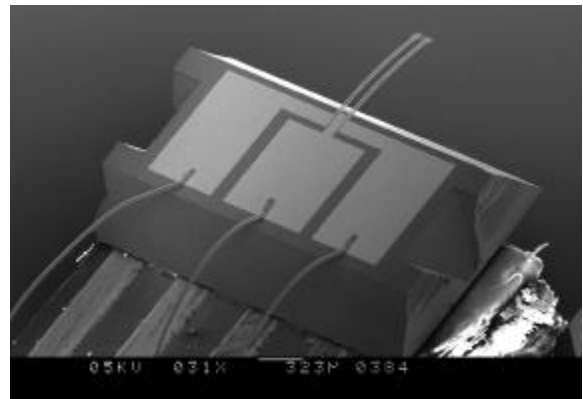


Figure 2 SEM photo of the structure

Figure 2 shows a realised microflown sensor. These sensors can be relatively easily produced in silicon micromachining technology delivering very robust, low-cost sensors.

## Theoretical description

The principle on which the present sensor is based, is the buoyancy, i.e. a combined presence of a fluid density gradient and a body force proportional to density. See e.g. [10]. In the present situation, the body force is the gravitation, whereas the density gradient is due to the temperature gradient, caused by the heating, see Figure 2.

In order to understand the properties of the sensor a description of the temperature profile around the two heaters and the flow velocities of the air is necessary.

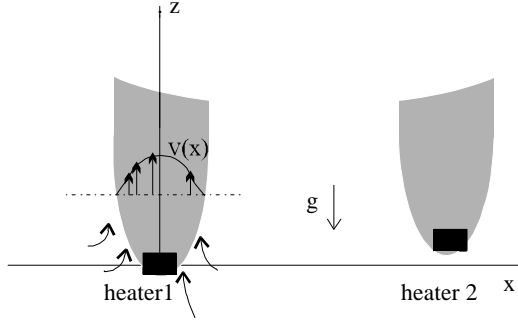


Figure 3: Schematic of the geometry under consideration

If initially only one infinitely long heater is considered, a heat balance, analogously to that given in [6] can be taken as starting point:

$$A \frac{\partial}{\partial y} \left( k_s \frac{\partial T_s}{\partial y} \right) + \frac{I^2 r_r}{A'} - rcA \frac{\partial T_s}{\partial t} - \mathbf{p} dh (T_s - T_f) - \mathbf{p} d\mathbf{se} (T_s^4 - T_f^4) = 0 \quad (1)$$

where  $k_s$  represents the thermal conductivity coefficient of the sensor material,  $A$  the cross section of the sensor and  $A'$  the cross section of the conducting part of the sensor,  $T_s$  its temperature,  $I$  the electrical current,  $r_r$  the resistivity of the sensor material,  $\mathbf{r}$  the density,  $c$  the specific heat,  $t$  the time,  $h$  the coefficient of convective heat transfer,  $T_f$  the temperature of the surrounding fluid,  $\mathbf{s}$  the Stefan-Boltzmann constant and  $\mathbf{e}$  the emissivity of the sensor. The first term of (1) corresponds to the heat transfer by conduction in the material, the second term to the electrical heat generation (the electrical power

per unit length  $P_{el}$ , [W/m]) and the third part to heat storage. The fourth term represents the loss by convection and conduction to the air, the last term the emission loss, which is usually neglected ([8], [9]).

If the temperature profile along the heater is assumed to be constant, which is justified if the heater is long compared to its width, the first term vanishes, and (1) reduces to

$$P_{el} = rcA \frac{\partial T_s}{\partial t} + \mathbf{p} dh (T_s - T_f) \quad (2)$$

In a critical analysis [7] it is argued that in the present configuration (and for the lengths and diameters used) and for the estimated velocities, it is incorrect to use the expression for  $h$  that is usually applied in anemometry (as well as in [4]). Besides, it is shown that  $\partial T_s / \partial t$  is negligibly small stressing the importance of  $h$ .

If, initially, only one heater is considered, the temperature of the fluid  $T$  and the velocities in  $x$ - and  $z$ -directions,  $u$  and  $v$  respectively, obey the following set of equations,

$$\frac{\partial u}{\partial x} + \frac{\partial v}{\partial z} = 0 \quad (4)$$

$$v \frac{\partial v}{\partial z} + u \frac{\partial v}{\partial x} = g\beta(T - T_\infty) + v \left( \frac{\partial^2 v}{\partial x^2} + \frac{\partial^2 v}{\partial z^2} \right) \quad (5)$$

$$u \frac{\partial T}{\partial x} + v \frac{\partial T}{\partial z} = \alpha \left( \frac{\partial^2 T}{\partial x^2} + \frac{\partial^2 T}{\partial z^2} \right) \quad (6)$$

with  $\mathbf{b}$  the volumetric thermal expansion coefficient,  $\mathbf{n}$  the kinematic viscosity,  $\mathbf{a}$  the thermal diffusivity and  $T_\infty$  the temperature of the fluid far from the heater. See Figure 3 and Figure 4.

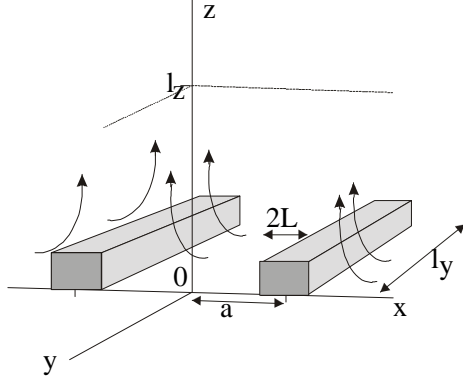


Figure 4. Dimensions of the model of the sensor

The first of the three coupled equations (4) is the continuity equation, the second (5) is obtained from the Navier-Stokes equation in which now the buoyancy force appears, where the third is the energy equation for the thermal problem. Since these equations are coupled, they can in principle be solved only simultaneously.

Following [4], it is justified to assume that for small velocities, the temperature distribution is independent of the velocity of the fluid (the air) and is only determined by the dimensions and power of the heaters and several coefficients like the diffusivity. This means that first a solution for  $T$  can be computed which then is substituted in the three coupled equations (4-6).

If we assume cold walls (ideal heatsinks) around the sensor at distances  $\pm l_y/2$  and  $\pm l_z$ , a solution for the temperature profile  $T(x,y,x)$  can be written as a series

$$T(x,y,z) = \sum_{n=0}^{\infty} \sum_{m=0}^{\infty} T_{nm}(x) \cos\left(\frac{\lambda_m 2y}{l_y}\right) \cos\left(\frac{\lambda_n z}{l_z}\right) \quad (7)$$

$$\lambda_m = \frac{\pi}{2}(2m+1)$$

where  $\cos(l_m 2y/l_y)$  and  $\cos(l_n z/l_z)$  are orthogonal functions,  $x$  is the horizontal distance perpendicular to the heater,  $y$  the distance along the heater and  $z$  the vertical direction. After normalisation to dimensionless coordinates, defining several constants [7], introducing a function that represents the heat sources, and solving the stationary heat flux equation with appropriate boundary

conditions, the coefficients  $T_{nm}$  are found

$$T_{nm} = \tau \begin{cases} Ae^{-\sigma_{nm}\xi} & \xi > \xi_1 + \xi_0 \\ 1 - Be^{-\sigma_{nm}\xi} - C \cosh(\sigma_{nm}\xi) & \xi_1 + \xi_0 < \xi < \xi_1 + \xi_0 \\ D \cosh(\sigma_{nm}\xi) e^{-\sigma_{nm}\xi_1} & 0 < \xi < \xi_1 - \xi_0 \end{cases}$$

(8)

with  $\tau$ ,  $A$ ,  $B$ ,  $C$ ,  $D$  constants defined by:

$$\tau = T_0 \frac{\pi(-1)^m}{\lambda_m \sigma_{nm}^2 \xi_0}$$

$$A = 2 \sinh(\sigma_{nm} \xi_0) \cosh(\sigma_{nm} \xi_1)$$

$$B = \sinh(\sigma_{nm} (\xi_1 - \xi_0))$$

$$C = -e^{-\sigma_{nm} (\xi_1 + \xi_0)}$$

$$D = 2 \sinh(\sigma_{nm} \xi_0)$$

Equation (8) is symmetric with respect to  $\xi=0$ , between both sensors.  $\xi_1$  is the normalised position  $x$  of the sensor,  $\xi_0$  its normalised width. If the interval between the heaters is considered, the third of equations (8) should be applied. In most cases, the first harmonic of the series (7) dominates, so that the temperature distribution in this area behaves approximately as

$$T(x,z) = c_T(z)(e^{m_1 x} + e^{-m_1 x}) \quad (9)$$

with  $c_T(z)$  a function independent of  $x$  and  $m_1$  a certain constant. Substitution of the expression for  $T(x,z)$  (9) into equation (6) yields equations for  $u(x,z)$  and  $v(x,z)$  only. Together with (4), a differential equation for  $u(x,z)$  with only first order partial derivatives of  $u(x,z)$  to  $x$  and  $z$  is obtained. This equation can in principle be solved, analytically or numerically. Since only the first harmonic in the expansion for  $T$  was considered, the  $z$ -dependence of  $T$  obeys  $c(z) \propto \cos(m_2 z)$ , where  $m_2 = \lambda_0/l_y = \pi/2l_y$ . This approach makes the solution of the partial differential equation in normalised coordinates for  $u(\mathbf{x},z)$  possible, after which, by application of (6), a complicated expression for  $v(\mathbf{x},z)$  can be found. After some manipulations it is seen that

$$u(\mathbf{x}, \mathbf{z}) = u_0(e^{m_1 x} + e^{-m_1 x} - 1)(1 - \sin m_2 z) \quad (10)$$

These equations are only a valid approximation for  $|x| < x_1 - x_0$ , i.e. in between both heaters. In principle, the value of  $u_0$  can be determined by substituting boundary values near the sensor. Calculations lead to

$$u_0 = \frac{m_2 \sqrt{((m_1^2 + m_2^2)(a+n) \sinh m_1(x_1 - x_0))^2 - gb\Delta T m_1(8 - \cosh m_1(x_1 - x_0))}}{(m_1^2 + m_2^2)(8 - \sinh m_1(x_1 - x_0))} \quad (11)$$

Assuming realistic, experimental, values for the variables in (11) we find  $u_0 = 0,24 \text{ m/s}$ .

Since calculated free and forced convection- and the associated Nusselt numbers- appear to be of the same order of magnitude, buoyance effects have strong influences and can be well measured with this configuration.

The aim of the set-up is to measure the angle between the plane of the two sensors and the horizontal plane. The sensitivity of this angle-measurement is determined by the rate of change of the horizontal (x) component of the velocity (which influences the heat transfer by convection) due to a slight variation of the z-position of one heater with respect to the other. It can be argued that the initial sensitivity is related to  $\partial u / \partial z$ , where the angle  $\phi$  equals  $z/2a$ . Using (10) and (11),

$$\frac{\partial u}{\partial z} = \frac{\partial u}{\partial z} \frac{\partial z}{\partial z} = \frac{m}{1_z} u = \frac{p}{2} \sqrt{\frac{1}{1_z^2} + \left(\frac{2}{1_y}\right)^2} \cdot u \quad (12)$$

This expression can be applied to optimise the sensitivity of the sensors.

## Measurements

Some preliminary measurements are done to demonstrate the operation principle of the level-sensor. From the temperature dependent resistance of the heaters the temperature difference can be obtained. The heaters are put in a Wheatstone bridge, see Figure 5, to obtain a high common signal rejection. Resistor R1 is fixed, R2 is adjustable to be able to zero the output voltage  $U_{out}$ . The resistance of the heaters are denoted as Rh1 and Rh2. The current through one heater is 2 mA, which gives a heat generation of 5.8 mW. Their spacing is 100  $\mu\text{m}$ . The structure

is placed in a box to prevent any forced convection. This has been done as well for the electronic circuit.

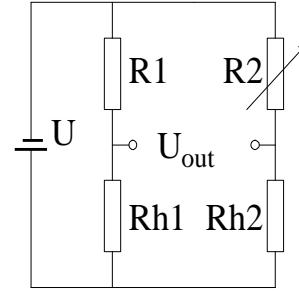


Figure 5 Electronic circuit with  $R1=390\Omega$ ,  $R2=0-1k\Omega$  and  $Rh1 \gg Rh2 \gg 350\Omega$ . and  $U=3V$ .

With a simple set-up the plane parallel to the beams is ramped up from horizontal to 90 degrees and to minus 90 degrees. For each angle the mean value of 100 measurement points is plotted in Figure 6. The standard deviation of the measurements was smaller than  $1\mu\text{V}$  and therefore error bars are omitted in the graph.

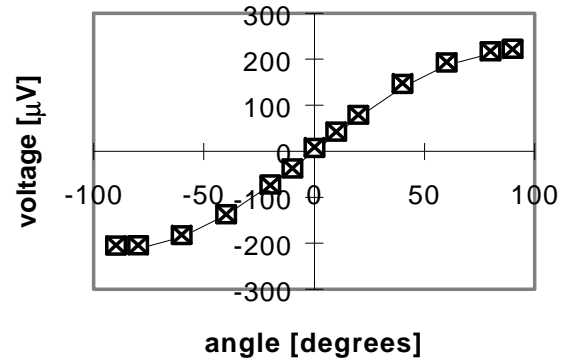


Figure 6 Output voltage versus angle relative to the horizontal.

The sensitivity of the level sensor is highest around the horizontal position, about  $3 \mu\text{V}/\text{degree}$ . The solid line is a fit of the measurement points using a least mean squares fit to a sine function.

From the difference in voltage drop over the both resistors we calculated the temperature difference of the beams (in vertical position) to be on the order of 50 mK. During experiments we noted a clear drift of the output voltage on the order of  $10 \mu\text{V}$  limiting the accuracy of the level-sensor to 3 degrees

around the horizontal position. We expect to be able to increase the accuracy by at least one order by using more advanced measurement methods. E.g. using AC signals drift signals can be considerably reduced.

### Conclusions

We have presented a novel level-sensor and shown first experiments demonstrating the viability of the sensor. Although accuracy was hampered by drift we expect that large improvements can be obtained using different measurement techniques. Owing to silicon micromachining techniques these sensors could be low-cost alternatives to more accurate and expensive level sensors.

### Acknowledgements

The authors like to thank I. Winter and V. Svetovoy of the *Institut fur Radiophysik, University of Jaroslwl* without whose work the theoretical model presented in this paper would not have been possible.

The research presented in this paper was made possible by the financial support of the Dutch Technology Foundation (STW).

### References

[1] Raatikainen P, Kassamakov I, Kakanakov R, Luukkala M, "Fiber-optic liquid-level sensor", *Sensors and Actuators A-physical*, 58: (2) 93-97

FEB 1997

[2] Werthschutzky R, Hagist K, "Level Sensor with digital signal-processing", *technisches messen*, 62: (11) 416-423 NOV 1995

[3] T.S.J. Lammerink et al, "Micro Liquid Flow Sensor," *Sensors and Actuators A*, pp.37-38, 45-50, (1993).

[4] H.E. de Bree et al, "The Microflown", *Sensors and Actuators A*, Physical, volume SNA054/1-3, pp 552-557, 1996.

[5] A. Leung, J. Jones, E. Czyzewska, J. Chen and M. Pascal, "Micromachined Accelerometer With No Proof Mass", IEDM, Washington, DC, December 7-10, 1997, p899-902.

[6] Fundamentals of hot wire anemometry, C.G.Lomas, *Cambridge University Press*, Cambridge, 1986

[7] Private communications, with prof. Dr. I. Winter, Dr.V.Svetovoy, Jaroslwl.

[8] R.Aigner et al, "SI-Planar- Pellistor Designs for temperature modulated operation", '95-Euroensors IX, 213-PD5

[9] Yang et. al., Monolithic flow sensor for measuring millimeter per minute flow, *Sensors and Actuators A*, 33, 1992, 143-153

[10] Fundamentals of heat and mass transfer, F.P.Incropera, D.P. deWitt, *John Wiley & Sons*, New York, 1990